# Effect of $Ca(OH)_2$ on the chemical precipitation of phosphates from solutions of a low concentration in fluidized bed reactor: hydrodynamic evaluation

# Effet de $Ca(OH)_2$ sur la précipitation chimique de phosphates à partir des solutions à faible concentration dans un réacteur à lit fluidisé: évaluation hydrodynamique

**Riad Eutamene *, Leila Benmansour *, Khashayar Saleh ****
* Environmental Engineering Laboratory, Process Engineering Department, University of Badji Mokhtar - Annaba, Algeria
** Industrial Process Engineering Department, CS60319, University the Technology of Compiegne, France

**Article Info**

***Article history:***

Received 31/10/2018
Revised 22/01/2019
Accepted 30/01/2019

***Keyword:***

Chemical precipitation - Fluidized bed - Phosphate - Porosity - Molar ratio.

**ABSTRACT**

In this present work, the phosphate is precipitated chemically at 22°C using synthetic water at different Ca/P molar ratios ranging from 0.5 to 12. Various parameters have been optimized to a range of realistic conditions relative to chemical precipitation of phosphates (superficial velocity of fluid $U_f$ = 0.58 cm/s, $[PO_4]$ = 10 mgP/L). A hydrodynamic evaluation of the chemical precipitation of phosphates in a fluidized bed reactor, contains sand particles as a substrate for the precipitate layer, from an ascending water stream using $Ca(OH)_2$ was made. As a function of Ca/P, the occurrences domains of the different hydrodynamics parameters are given. The effect of the $Ca(OH)_2$ on the porosity and the velocity of the fluidized bed it also presented. For the inlet Ca/P molar ratio, was lower than 4, the phosphate removal efficiency is 35~74%. While, for the suitable conditions of Ca/P>4, the phosphate removal efficiency ranging from 75 to 92%. It is found that the [Ca] and $[PO_4]$ significantly affect the velocity of fluidization and the porosity of the fluidized bed. In this connection, the experimental data of several authors provide a useful starting point for our comparisons.

***Mots-clés :***

Précipitation chimique - Lit fluidisé - Phosphate - Porosité - Rapport molaire.

**RÉSUMÉ**

Dans ce travail, le phosphate est précipité chimiquement à 22°C en utilisant de l'eau synthétique à différent rapport molaire Ca/P allant de 0.5 à 12. Différents paramètres ont été optimisés pour une gamme de conditions réalistes relatives à la précipitation chimique des phosphates (vitesse superficielle du fluide $U_f$ = 0.58 cm/s, $[PO_4]$ = 10 mgP/L). Une évaluation hydrodynamique de la précipitation chimique des phosphates a été étudiée dans un réacteur à lit fluidisé qui contient de sable comme des particules porteuses de la couche précipitée, à partir d'un courant d'eau ascendant utilisant du $Ca(OH)_2$. En fonction de Ca/P, les domaines d'occurrence des différents paramètres hydrodynamiques ont été donnés. L'effet du $Ca(OH)_2$ sur la porosité et la vitesse du lit fluidisé a été présenté également. Pour un rapport molaire Ca/P inférieur à 4, l'efficacité d'élimination du phosphate est de 35 à 74%. Alors que, pour les conditions appropriées de Ca/P > 4, l'efficacité d'élimination du phosphate varie de 75 à 92%. On constate que les concentrations [Ca] et $[PO_4]$ affectent de manière significative la vitesse de fluidisation et la porosité du lit fluidisé. À cet égard, les données expérimentales de plusieurs auteurs constituent un point de départ utile pour nos comparaisons.

***Corresponding Author:***
Riad Eutamene,
Environmental Engineering Laboratory, Process Engineering Department, University of Badji Mokhtar - Annaba, Algeria
Email: athameneriad@yahoo.fr

## 1. INTRODUCTION

Phosphates considerate similar to a pollution index, can be a problem at high concentration in the environment [1], [2]. Their presence in the water at high concentrations (≥ 0.1 mgP/L) causes precipitation of crystalline phosphates in wastewater systems, which leads to the eutrophication of rivers, lakes and of the world's seas [3], [4]. In an attempt to improve the water quality of the lakes, and in order to try to control the eutrophication of the river, several authors have looked to reduce the phosphates concentrations in the industrial wastewater [1], [5]-[9]. Phosphates removal techniques include chemical precipitation [10]-[12], biological treatment [2], [6], [13] and crystallization [1], [14]. The chemical precipitation of the phosphates as a calcium salt from the water and wastewater in a fluidized bed reactor (FBR) has been the subject of intensive research [4], [10], due to their importance in different fields, like industry, environment and health [9]. Removal of the calcium phosphate in the fluidized bed reactor (FBR) by chemical precipitation is an effective alternative to the other approved methods. For this purpose, we adopted the process of chemical precipitation in this work. The main focus of this study is the evaluation of a proper experimental method for the recovery of phosphates through a hydrodynamic approach. The use of chemical precipitation to remove the phosphates depending on the process and operating conditions [9]. In this study, the first screening study was completed for fluidized bed process with low inlet phosphate concentration by varying operating conditions such as the concentration of $Ca(OH)_2$ and the outlet pH, to vary Ca/P values between 0.5 at 12. Farther, the features of the process such as the phosphate removal efficiency and mechanical stability of the phosphate grains were determined. The effect of some impurities in water or in precipitation materials such as magnesium and carbonates, which can interfere with the process, has also been discussed. The effects of pH and the molar ratio on phosphate removal were also examined. It is also studied the effect of $Ca(OH)_2$ concentration on the relationship between the liquid and solid phase's (water and grains).

## 2. PRECIPITATION AND FLUIDIZATION

### 2.1. Chemistry of calcium phosphate removal

The precipitation of calcium phosphate strongly depends on the pH of the solution and the concentration of the mixing solutions [9], [12]. The solubility of calcium phosphates is a function of these parameters. By dosing calcium in the water and adjusting the pH, the solubility of calcium phosphates is exceeded and calcium phosphate is recovered by chemical precipitation from water to the solid phase. Today, the calcium phosphate is obtained upon seed material grains. The precipitation of the calcium phosphate is based on the mixing of the phosphate solution with the calcium. The mixing provides to shift to the left in the chemical equilibrium given in equations (1-3) [15] :

$$H_3PO_4 \leftrightarrow H_2PO_4^- + H^+ \quad (1)$$

$$H_2PO_4^- \leftrightarrow HPO_4^{2-} + H^+ \quad (2)$$

$$HPO_4^{2-} \leftrightarrow PO_4^{3-} + H^+ \quad (3)$$

Because of these reactions, precipitation leads to increased acidity, therefore, the saturation decreases rapidly. In the precipitation technique, when phosphate and calcium occur in water, the calcium phosphate will be formed in different phases (hydroxyapatite (HAP, $Ca_5(PO_4)_3(OH)$, Bruchite (DCPD, $CaH(PO_4).2H_2O$), tricalcium phosphate (TCP, $Ca_3(PO_4)_2$ and amorphous calcium phosphate (ACP, $Ca_9(PO_4)_6.xH_2O$)) under different conditions as given by the reactions below:

$$5Ca^{2+} + 3PO_4^{3-} + OH^- \leftrightarrow Ca_5(PO_4)_3(OH) \quad (4)$$

$$4Ca^{2+} + H^+ + 3PO_4^{3-} + 3H_2O \leftrightarrow Ca_4H(PO_4)_3.3H_2O \quad (5)$$

$$3Ca^{2+} + 2PO_4^{3-} \leftrightarrow Ca_3(PO_4)_2 \quad (6)$$

$$Ca^{2+} + HPO_4^{2-} \leftrightarrow CaH(PO_4) \quad (7)$$

$$Ca^{2+} + HPO_4^{2-} + 2H_2O \leftrightarrow CaH(PO_4).2H_2O \quad (8)$$

The lime is the most common calcium salt used for calcium phosphate precipitation, to provide simultaneous increases in both calcium and hydroxyl ion [2]. This precipitation usually occurs within the pH range 7 to 11 [12]. Seckler et al. [10] used the $Ca(OH)_2$ and NaOH to recover phosphates from water model contain a phosphate in a concentration range between 5 and 100 mgP/L, with continuous-flow FBR. They are found that the efficiency of 56% was achieved. Generally, sand grains were used as seeds material in various precipitation processes [10], [15].

**2.2. Data analysis**

The efficiency of phosphate removal ($\eta$) and the conversion ($\chi$) are given by the following equations [9], [16], [17]:

$$\eta = 100.\left(\left[PO_4^{3-}\right]_{in} - \left[PO_4^{3-}\right]_{out}\right)/\left[PO_4^{3-}\right]_{in} \quad (9)$$

$$\chi = 100.\left(\left[PO_4^{3-}\right]_{in} - \left[PO_4^{3-}\right]_{sol}\right)/\left[PO_4^{3-}\right]_{in} \quad (10)$$

In which:
$[PO_4^{3-}]_{in}$ is denotes the initial phosphate concentration at the reactor inlet , mgP/L.
$[PO_4^{3-}]_{out}$ is denotes the total phosphate concentration in the column out of the reactor (without filtration), mgP/L.
$[PO_4^{3-}]_{sol}$ is denotes the solute phosphate concentration at the reactor outlet (with filtration), mgP/L.

These parameters are also good indicators of the phosphate removal and provide important information on the precipitation process. The difference between the efficiency of the precipitation and the efficiency of the recovery is the fines crystals loss in the reactor effluent (Fig. 1).

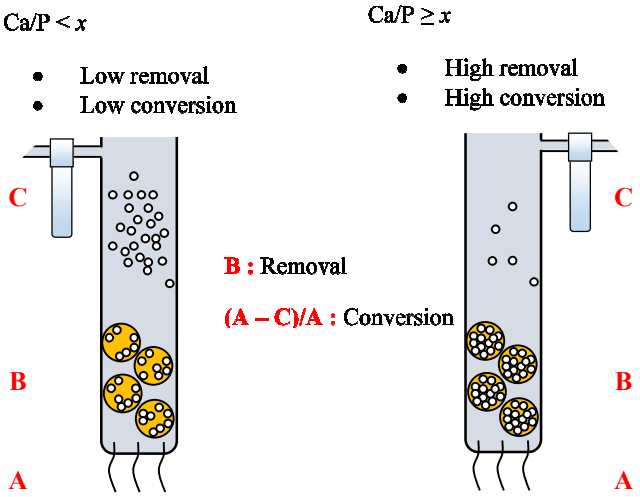


Figure 1. Influence of the molar ratio Ca/P on the conversion and the removal efficiency of phosphates [18].

On the other hand, the behavior of the chemical precipitation by a hydrodynamic evaluation has not been investigated. Furthermore, the relation between the porosity of the bed and the efficiency of removing the phosphates has not yet been established.

When the particles are supported by the fluid in a fluidized bed, we can write [19]:

$$\Delta P.A = \left(M/\rho_s\right)\left(\rho_s - \rho\right)g \quad (11)$$

This relation can also be written in the form:

$$\varepsilon = 1 - \left(\Delta P/H\left(\rho_s - \rho\right)g\right) \quad (12)$$

Where A is the cross-sectional area of the bed ( $A = \pi r^2$ ), M is the mass particles within the reactor and $\Delta P$ is the pressure drop. H is the height of the bed and ε is the porosity of the bed. $\rho_s$ and ρ are density of solid particles and fluide, respectively. The expansion of the fluidized bed ($H/H_{mf}$) is defined experimentally as the fraction between the average porosity and the porosity at the minimum of fluidization.

The relation between the porosity and height of the bed takes the following form [20]:

$$H = a - b\left[\begin{array}{l} 2\ \varepsilon^{-0.5} + \frac{1}{1.5}\varepsilon^{-1.5} + \frac{1}{2.5}\varepsilon^{-2.5} \\ + \frac{1}{3.5}\varepsilon^{-3.5} + \varepsilon^{-4.5} - \ln\left(\frac{1+\sqrt{\varepsilon}}{1-\sqrt{\varepsilon}}\right) \end{array}\right] \quad (13)$$

Where *a* and *b* are coefficients require experimental values of the height H of the bed.

The velocity of the fluidization of the particles is determined as [21]:

$$U_f = w/A \quad (14)$$

Where *w* is the fluid flow rate.

## 3. MATERIALS AND METHODOLOGY

We prepared a stock solution of phosphate using $Na_2HPO_4.H_2O$ (Verbière, France) as a phosphate source of 1000 $mgPO_4^{3-}$/liter of distilled water, and left in a thermostatically controlled room (22°C). $Ca(OH)_2$ (Verbièse, France) is used in the form of a 1000 mg/L stock solution, maximum impurities: $Al_2O_3$: 0.17 %, $Fe_2O_3$: 0.21%, MgO: 0.9%, $SiO_2$: 0.8 %, S: 0.035 %. The pH was adjusted by using a NaOH (Verbièse, France) with sodium bicarbonate in the form of a buffer solution (carbonate content: $Na_2CO_3 \leq$ 0.4 %) to have a pH 9.6 value.

The phosphate solutions used are synthesized with a total content of 10 mgP/L of city water (the concentration of $PO_4$ is always expressed as the phosphorus content of dihydrogen phosphate, 1 mgP-$PO_4^{3-}$/L corresponds to 3.07 $mgPO_4^{3-}$/L). With the addition of the phosphate concentration of 2.46 mgP/L of city water, we will arrive at a total concentration of 12.5 mgP/L. The physicochemical parameters of water, as determined using standard method (APHA, 1985), are listed in table 1.

A FBR, 5 cm in diameter and a total high column of 145 cm, was used (Fig. 2). The precipitation was made in a continuous-flow FBR. The flow rate adapted is 36 L/h. The column is filled with 0.4 kg quartz sand particles (CV32, SIBELCO - France) as a carrier of precipitating substances, to obtain an expansion of 16 cm.

Table 1. Physicochemical characteristics of water used.

| Parameters | Values |
|---|---|
| pH | 7.4 |
| $[PO_4^{3-}]$ (mgP/L) | 2.46 |
| $[Mg^{2+}]$ (mg/L) | 21 |
| $[Ca^{2+}]$ (mg/L) | 106 |
| $[Cl^-]$ (mg/L) | 0.36 |
| $[NH_4^+]$ (mg/L ) | <0.05 |
| $[NO_3^-]$ (mg/L) | 25.1 |
| Conductivity at 20°C (µs/cm) | 710 |

The mean diameter of the quartz sand particles used is 220 µm (denoted Si-220). The average density is 2.4. The porosity (ε) and velocity at the minimum of fluidization ($U_{mf}$) of sand are 0.56 and 0.08 cm/s, respectively. All experiments were conducted at room temperature 22 °C. Each time a new amount of sand is used. The sand after each experiment has undergone drying as well as storage conditioning.

In the process of phosphate recovery, dephosphatation was optimized. Sand particles were used as a filter and substrate material. The first pump P-1 (Fig. 2) of the synthesized phosphate solution is first ignited with a low fluidization velocity (<$U_{mf}$), the sand particles have been then added from the upper part of the FBR. The fluid flow rate is increased to an average value equivalent to $U_{mf}$. The pH of the solution was monitored at ± 0.1 unit throughout the experiment by P-3 (Fig. 2) injection of a buffer solution. You can then set the velocity of injections to 7.$U_{mf}$. After the stabilization of pH solution, the $Ca(OH)_2$ solution was added continuously using a P-2 pump (Fig. 2). Finally, the process of the precipitation starts.

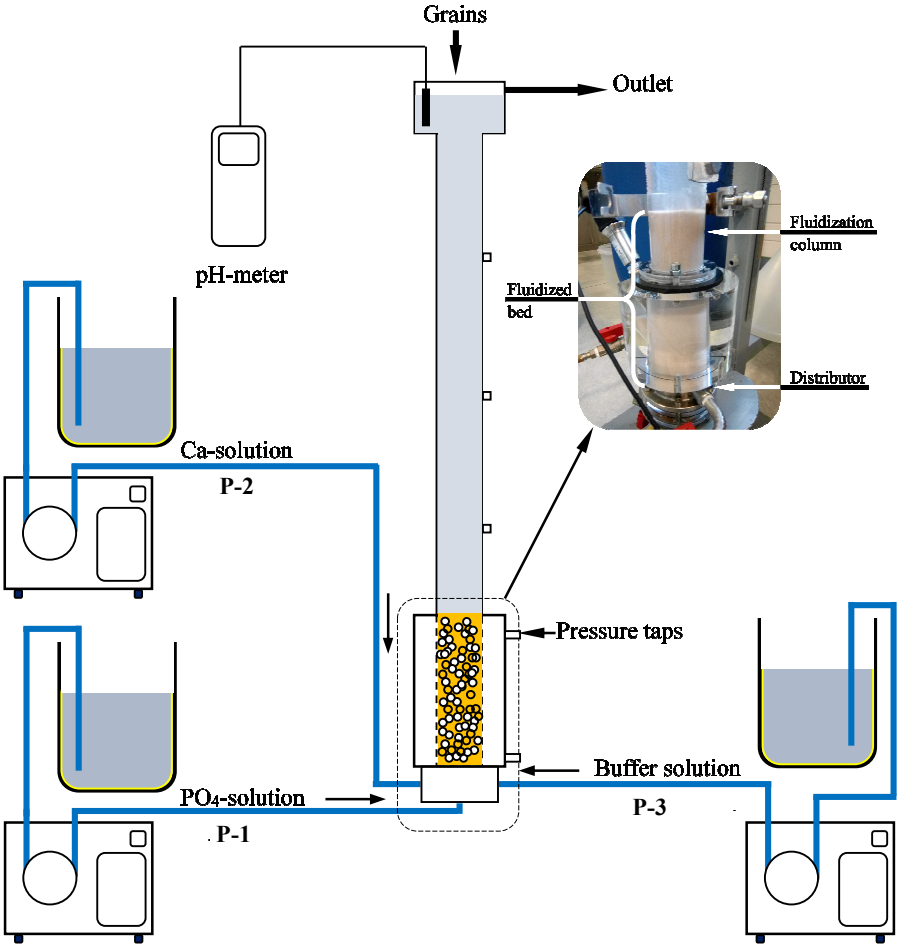


Figure 2. Schema of the FBR.

Daily simples extracted were taken at selected intervals and analyzed, injected immediately with a NaOH solution to stop the reaction [1]. Phosphate concentration was determined by a spectrometer (*Perkin Elmer Lambda 25 UV- Vis*). The pH was determined by using an *ALMEMO* pH meter model *2590-3S*. The sand after each experiment is removed from the reactor, dried at 60°C for 12 h and analyzed by scanning electron microscopy (SEM) (*FEI HP 3600*) and by FTIR to determinate possible Ca-phosphate compounds on the surface of individual particles of the carrier material.

## 4. RESULTS AND DISCUSSION

The main parameters whose effects are to be evaluated are the phosphate removal efficiency, the velocity of the fluidization and the porosity of the bed, which contains the exchange rate between the solid phase and the solution of phosphate.

### 4.1. Effect of Ca-concentration in the phosphate removal efficiency

At the first approach to real conditions for the elimination of phosphates by the $Ca(OH)_2$ in FBR using a model water of 10 mgP/L, we chose to perform eight experiments with a range of realistic conditions compared to chemical precipitation of phosphates, by changing the molar ratio Ca/P values. Figure 3 (a) shows the mean value of the phosphate removal efficiency of chemical precipitation as a function of time for the eight configurations studied.

By the use of Ca/P to 0.5 at 12, the efficiency of the $PO_4$-precipitation by $Ca^{2+}$ ions increased considerably from 40 to 92%, respectively.

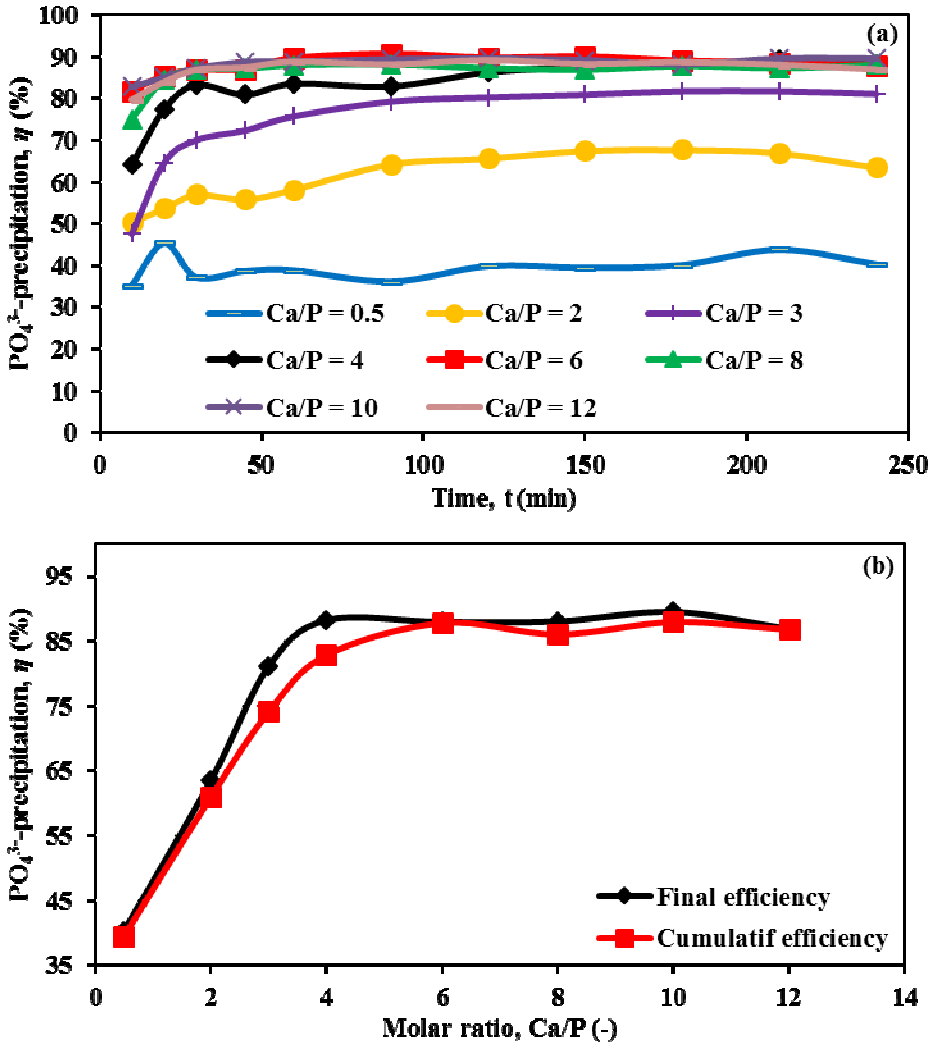


Figure 3. **a**) Evolution of the phosphate removal efficiency as a function of the time, **b**) Evolution of final and cumulative phosphate removal efficiency as a function of the molar ratio Ca/P ($[PO_4^{-3}]$ = 10 mgP/L , flow rate of 36 L/h, M = 0.4 kg).

These curves are similar in tendancy: a rapid increase in removal efficiency in the first thirty minutes followed by a slight increase until the second hour of the experiment, which ends with a constant evolution of the removal efficiency as a function of time, with the exception of the low molar ratio of 0.5 (Fig. 3 (a)). Thus, from the second hour of manipulation the influence of time appears to be insignificant and the removals efficiencies are constant (Fig. 3 (a)).

In order to establish the precipitation of calcium phosphate, the cumulative efficiency was investigated (Fig. 3 (b)). The cumulative yield is the mass of precipitate, which accumulates with time compared to the total precipitated mass at the end of the experiment. The evolution of the removal efficiency of chemical precipitation at different molar ratios is shown in figure 3 (b).

From the results obtained, we can see that the increase in the concentration of the $Ca(OH)_2$ in the FBR is accompanied by an increase in the removal efficiency of the recovery and the chemical precipitation of the phosphates is reached at 92% for a Ca/P-10, a standard deviation of 0.02 and an uncertainty of 0.01 (Fig. 3 (b)). $PO_4$-precipitation evidenced is better than that previously reported by Seckler et al. [10]. This difference can be attributed to the operative conditions employed.

The evolution of the phosphate removal efficiency as a function of the Ca/P, confirms that the latter has a significant influence on the removal efficiency. For effective removal of phosphates, the addition of calcium must be high enough to buffer the solution, with acidic solutions; the concentration of $Ca(OH)_2$ has to be adjusted. The solubility of $Ca(OH)_2$ is 1.73 g/L of water at a temperature of 20°C. From Ca/P-6, there is a saturated state of the calcium molecules in the solution. Otherwise, $Ca(OH)_2$ particles dissolve slowly along the bed length, distributing the supersaturation more evenly throughout the bed, and thus favoring growth upon the grains and aggregation of developed fines with the grains [10]. The growth of the residual phosphate concentration in the FBR as a function of the initial calcium concentration can be explained by the following points:

- $Ca/P < 2$ $pH < 8.3$

For low concentrations of $Ca(OH)_2$, a low pH is obtained which generally leads to the precipitation of a small amount, in the first hand, of calcium dihydrogen phosphate at low pH values (6 to 7) and that's not the case for us. As well as, the calcium dihydrogen phosphate has a fairly high solubility. On the other hand, for the low calcium concentrations (inlet molar ratio $Ca/P < 0.8$), and to the presence of magnesium current which can replace the lack of calcium and given which efficiency comparable to those of calcium from $Mg/PO_4$-precipitation [2], [10].

- $2 \leq Ca/P \leq 4$ $8.3 \leq pH \leq 9.3$

These conditions generally result in the formation of amorphous calcium phosphate ACP ($Ca_3(PO_4)_2$) at an optimum pH of 7.4 to 9 and Ca/P-1.5 [22] or hydroxyapatite $Ca_5(PO_4)_3OH$ at an optimum pH of 7.4 to 9 and Ca/P-1.33 or Ca/P-1.67 [23], [24].

- $4 < Ca/P < 10$ $9.3 <pH < 10.1$

For a pH above 9, the conditions are favorable for the precipitation of the HAP and TCP with a high excess of calcium which favors the precipitation [12]. This explains the increase in precipitation of phosphates in an FBR. The highest efficiency of phosphate precipitation was at the optimum pH of 9.6 (Ca/P-6).

- $Ca/P \geq 10$ $pH > 10.1$

For a molar ratio of 12, there may be a small decrease in the phosphate removal efficiency. This may be due to the concentrations of impurities of magnesium Mg and carbonate $CO_3$ in the bed. At certain Mg content and $CO_3$, the removal efficiency is decreased slowly [10], [25], [26]. Carbonate and magnesium ions tend to co-crystallize as calcium carbonate $CaCO_3$ and magnesium phosphate $MgHPO_4$ upon the grains of sand, and magnesium phosphate precipitates instead of calcium phosphate. The co-crystallization has been found to be associated with a reduction in the calcium phosphate removal efficiency [10]. But at pH values the formation of magnesium phosphate is not complete, and virtually complete at pH 11. Furthermore, in order to prevent fine particles formation and increase the efficiency of the process, the calcium concentration at the bottom of the reactor has to be kept below a critical value. This explains the slight diminution of the phosphate removal efficiency with the excess of $Ca(OH)_2$. Our results are in agreement with the results of Yigit et al. [12].

The experiments carried out showed that the Ca/P molar ratio of the mixture to a significant influence on the conversion and the efficiency of the fluidized bed (Fig. 4). The conversion at the reactor is an important component for phosphate removal. The optimum conversion corresponding to the maximum efficiency operates the fluidization of the calcium phosphate between 98.6 and 99.6 % (Fig. 4). Under these operating conditions, our results are in agreement with the results of Seckler et al. [10].

An increase in the total concentration of the $Ca(OH)_2$ results a shift to the right in the conversion and phosphate efficiency as a function of the pH curve. The final pH in the fluidized bed varies from 7.9 to 10.1 depending on the increase in $Ca(OH)_2$ concentration in the mixture in an average ratio $pH_{Ca}/pH_{Bed}$=1.32.

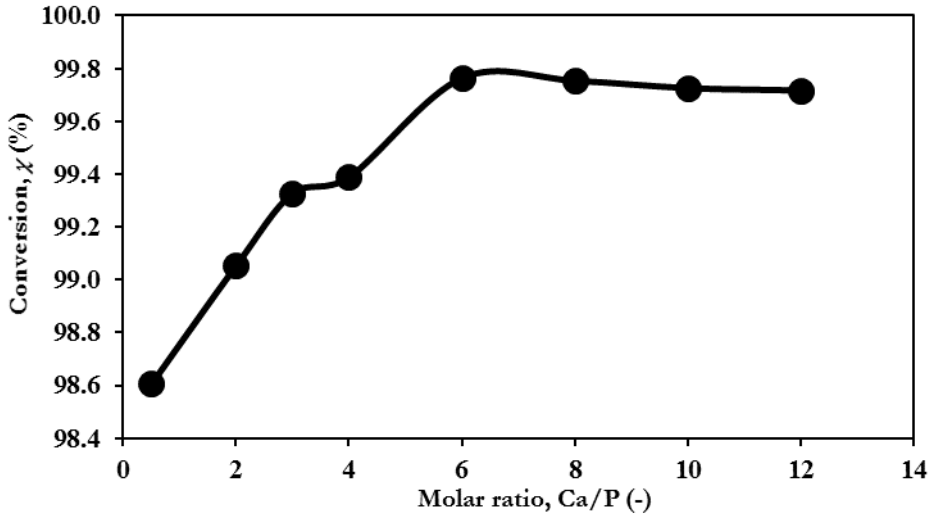


Figure 4. The conversion as a function of the molar ratio Ca/P ($[PO_4^{-3}]$ = 12.5 mgP/L, flow rate of 36 L/h, M = 0.4 kg).

The efficiency and conversion values measured at the outlet of the FBR are dominated by the pH values within the bed.

**4.2. Effect of Ca-concentration on different hydrodynamic parameters**

In this study, we are examining effects not studied on precipitation process in FBR (e.g. porosity of the bed and velocity of fluidization). In order to identify the effect of the Ca/P on the various hydrodynamic parameters, all of the parameters were determined, such as bed expansion, porosity and thus the velocity of fluidization. The decrease in the Ca/P of the mixture to effect on the rate of expansion; the latter is lower when the Ca/P ratio is equal to 0.5 and the amount of solid recovered after 4 h is weaker. This corresponds to slightly improved phosphate removal efficiency in the fluidized bed. The evolution of the bed height as a function of time is shown in the following figure 5 (a).

The increase in the top surface of the fluidized bed is almost constant for a molar ratio of Ca/P-6, and the expansion value reaches up to double, with a maximum standard deviation of $3.4.10^{-4}$ and an uncertainty of $8.10^{-4}$ for a molar ratio Ca/P-12 (Fig. 5 (a) and Fig. 5 (b)).

At a temperature of 22°C and a pH 7.9~10.1, our experiments confirm the influence of Ca/P on the expansion of the fluidized bed. From Ca/P-6, the quantity of phosphate rejected is less than 1.9 mgP/L and the precipitate is completely retained in the FBR. The concentration of $PO_4$ in the outlet of FBR was lower than in pure water. For the above curve, the evolution of the expansion as a function of Ca/P is the same, a rapid increase of the $H/H_{mf}$ for the first Ca/P-values up to a maximum value of Ca/P-6, which follows by a constant value. For Ca/P-6, there is a maximum expansion of 2 with a maximum standard deviation of $0.2.10^{-3}$ and an uncertainty of $0.7.10^{-3}$.

The granulometric distribution also changes with advancing precipitation, the only parameter that can provide an image on this change is the porosity of the bed. The porosity is represented by the void between the carrier particles. If this void is filled with fine particles, results in a decrease in porosity, the latter is confirmed by the following curve (Fig. 6 (a)). In the literature, studies on the analysis and determination of porosity of fluidized bed precipitation are scarce.

To the last of our knowledge, the porosity has not yet been studied in the chemical precipitation of phosphates. This is the first time that this parameter has been introduced, as well as the velocity of fluidization.

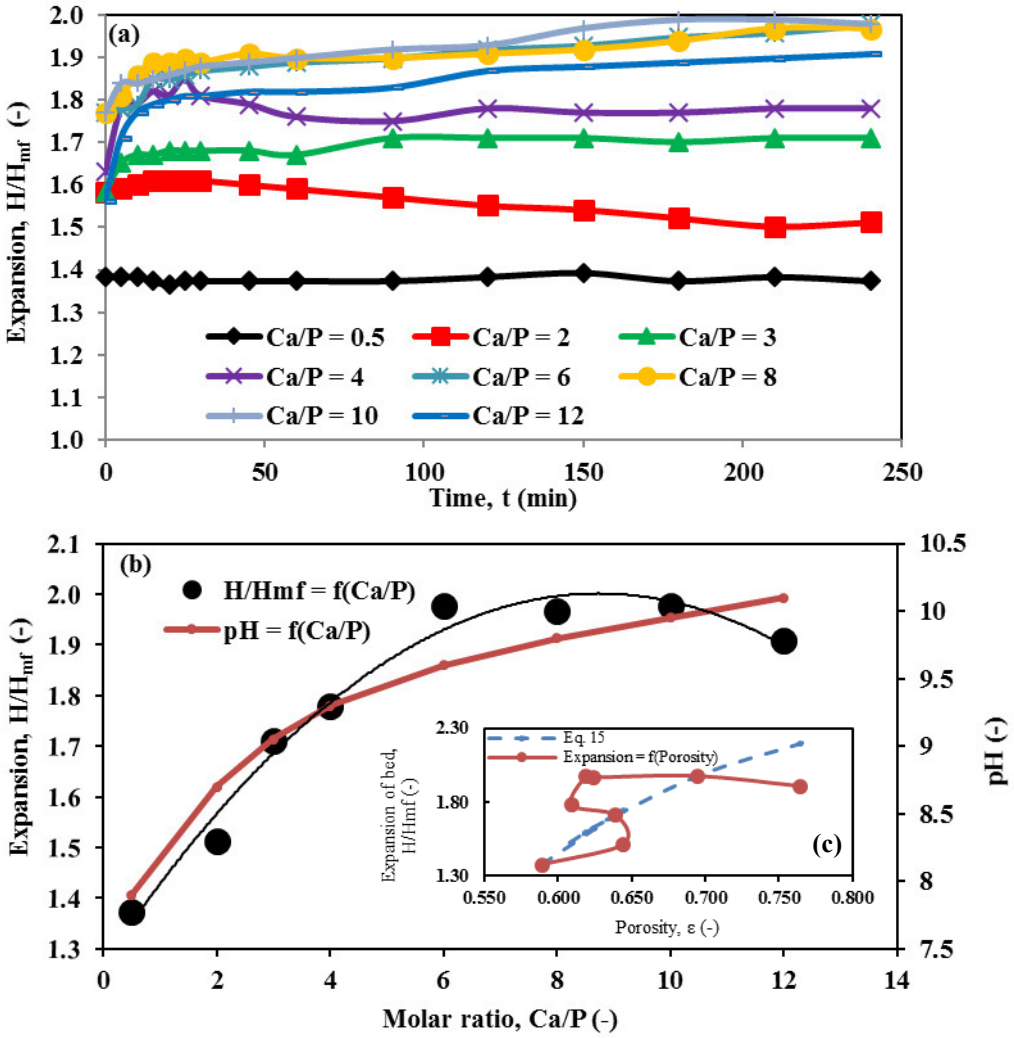


Figure 5. **a**) Change of expansion as a function of the time, **b**) Change of the expansion as a function of Ca/P, **c**) Change of the expansion as a function of porosity (flow rate of 36 L/h, $[PO_4^{-3}]$ =12.5 mg P/L, M = 0.4 kg).

In this context, the porosity results of the various values Ca/P for a constant concentration of phosphate 12.5 mgP/L are shown in figure 6 (a) and figure 6 (b).

Figure 6 (a), shows the porosity as a function of time, a zone of fluctuations which becomes important for a molar ratio equal to 3, followed by a slight decrease in the porosity as a function of time. These oscillations of the porosity on these curves for the first hour of manipulation can be attributed to the change of the structure of the bed due to the entrainment on the surface of the bed of the fine particles trapped by the large particles. These oscillations disappear at a fluidization time greater than 1 hour and thus ending in a constant porosity. In spite of this, an evolution of the porosity has been found with the molar ratio of an exponential form (Fig. 6 (b)). From the determination of exponent *a*, and *b* of equation 13. A new correlation of the determination of the expansion from fluidized bed porosity can be proposed for the precipitation process, as follows:

$$H/H_{mf} = 2.62 - 0.08\begin{bmatrix} 2\,\varepsilon^{-0.5} + 0.66\varepsilon^{-1.5} \\ +0.4\varepsilon^{-2.5} \\ +0.28\varepsilon^{-3.5} + \varepsilon^{-4.5} \\ -\ln\left(\dfrac{1+\sqrt{\varepsilon}}{1-\sqrt{\varepsilon}}\right) \end{bmatrix} \quad (15)$$

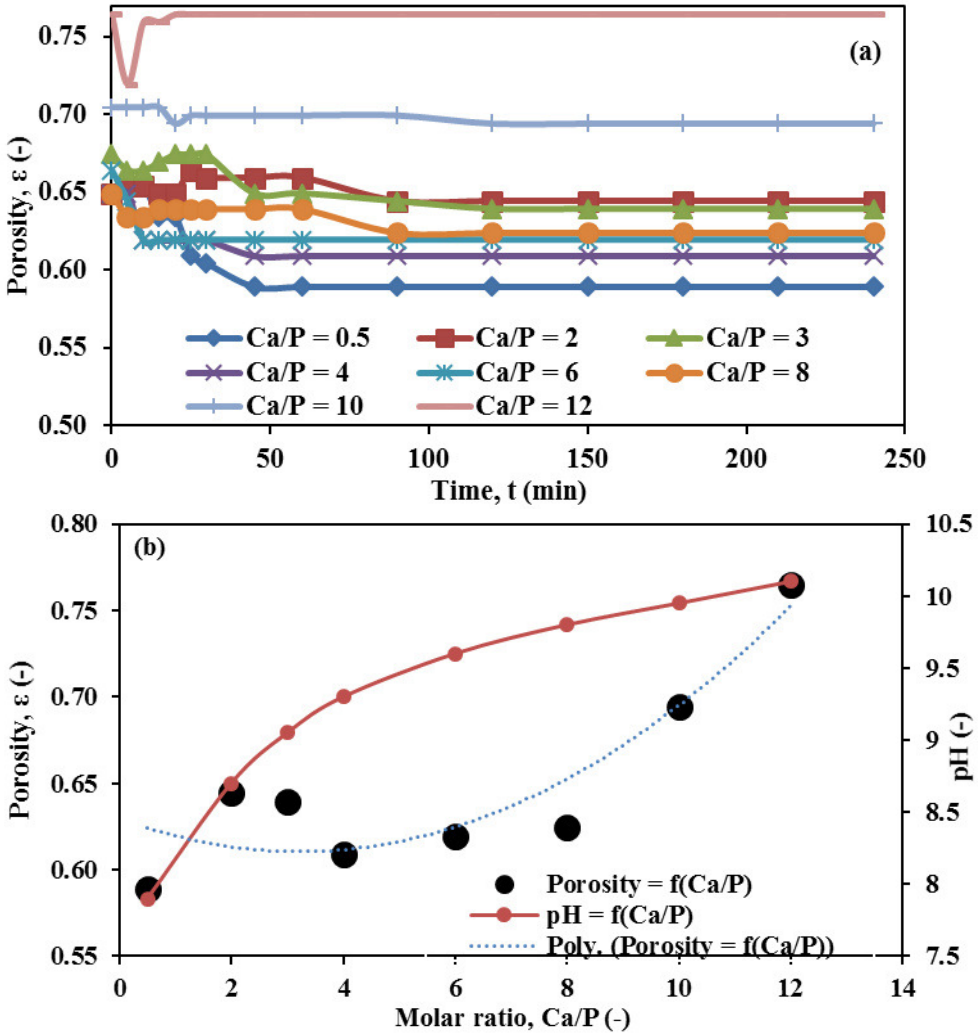


Figure 6. **a**) Evolution of the porosity of the bed as a function of the time, **b**) Evolution of the porosity of the bed as a function of the molar ratio ($[PO_4^{-3}]$ = 12.5 mgP/L, flow rate of 36 L/h, M = 0.4 kg).

In our conditions, the error of equation 15 does not exceed 10% (Fig. 5 (c)).

As an illustration, the fine particles formation with increasing the inlet molar ratio in the solution results by the decreasing of the average diameter of the binary mixture including course and fine particles. It is found that, the porosity decreases to a minimum for a molar ratio equal to 4, and then it increases with increasing of the inlet molar ratio and the increasing of fine particles formation. The same trend was observed by Formisani et al. [27] for a binary mixture of particles (Fig. 6).

Figures 7 (a) and 7 (b) shows the evolution of the velocity of the fluidization as a function of time and molar ratio, respectively. It is clearly seen that there is always an increase in the velocity of the fluidization as a function of the Ca/P for the eight configurations studied from 0.557 to 0.584 cm/s, indicating that the average diameter of the particles $d_p$ is slightly increased.

Moreover, the increase in the velocity of fluidization exhibits an exponential increase as a function of the inlet molar ratio, with a maximum standard deviation and an uncertainty of $0.2.10^{-4}$. As the average diameter of particles of seed material increases, the expansion ration of the fluidized bed increases, increasing the surface area of the seed per reactor volume and increasing the superficial velocity. In these conditions, the removal efficiency is higher.

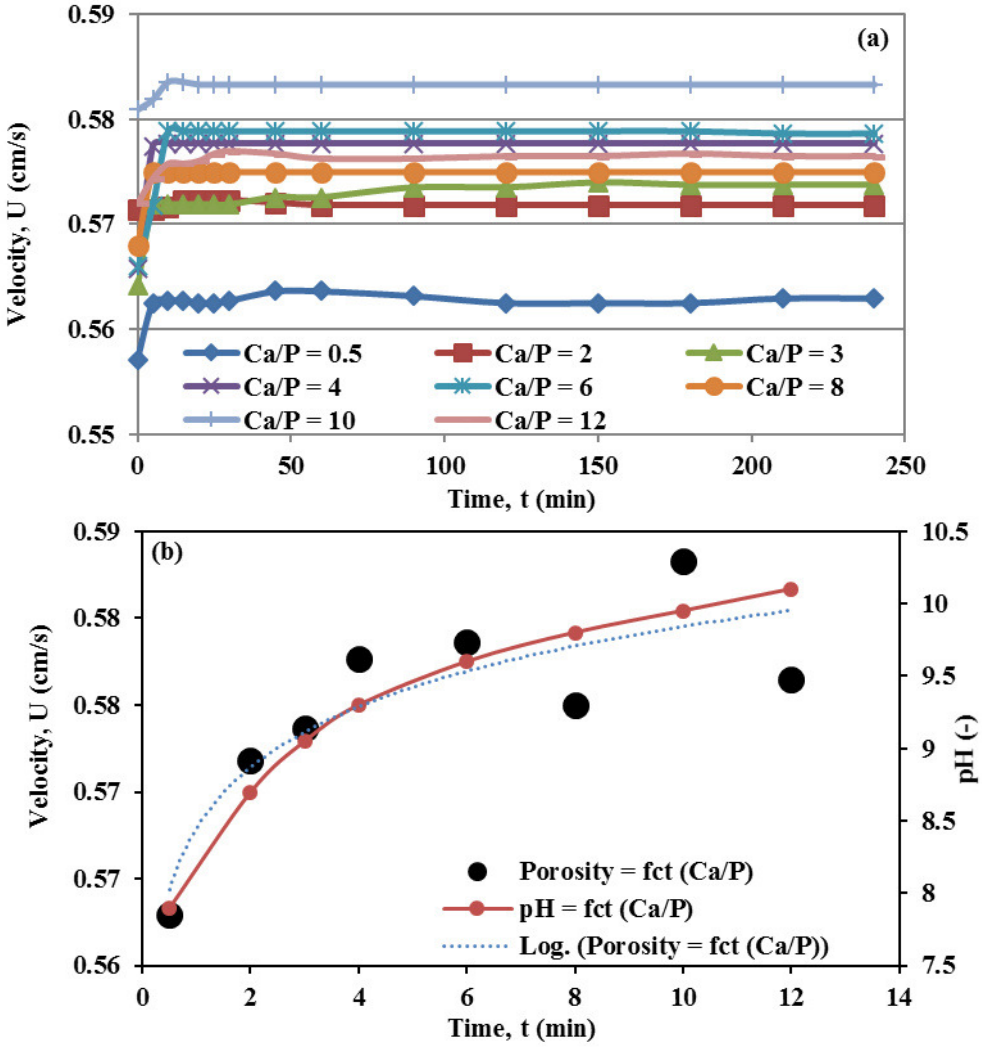


Figure 7. **a**) Evolution of the velocity of fluidization as a function of the time, **b**) The velocity of fluidization as a function of the molar ratio ($[PO_4^{-3}]$ = 12.5 mgP/L, flow rate of 36 L/h, M = 0.4 kg).

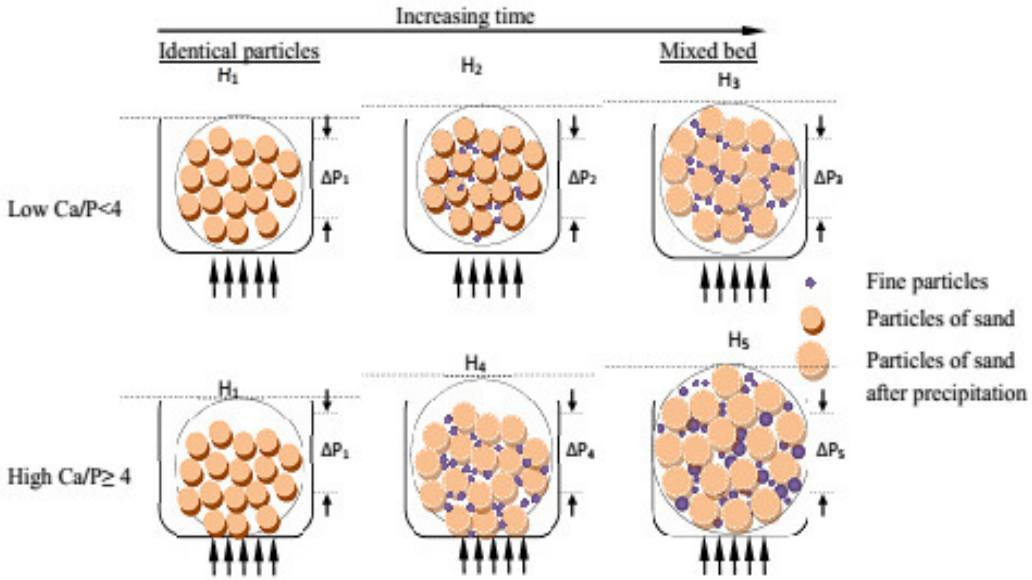


Figure 8. Influence of the molar ratio Ca/P on the hydrodynamic parameter in the fluidized bed reactor.

Figure 8 shows the influence of the molar ratio in the different hydrodynamics parameters. Furthermore, in order to prevent fine particles formation and increase the efficiency of the process, the calcium concentration at the bottom of the reactor has to be kept below a critical value.

Owing to the change of superficial velocity and the average diameter of particles, the porosity of the fluidized bed changes also (Fig. 8). At higher calcium concentrations, the formation of the fine particles which escape from the column favors the decrease of the removal phosphate efficiency (Fig. 8).

**4.3. Properties of the solids**

The observation of the following figures shows an increase in the average diameter $d_p$ of the particles during the manipulation, which confirms a good coating (Fig.9 (a) and Fig. 9 (b)). The surface is therefore covered by a strongly layer of solution molecules, and the thickness of the layer is 30 µm for a Ca/P-10. From the particles size distribution of the sand particles shown in figure 9 (a) before and after the precipitation, clearly shows that the $d_p$ of the particles is significantly increased from 220 µm to 279 µm. SEM analysis shows that the precipitated solid has an apatitic structure and fairly well crystallized, and has a molar ratio Ca/P determined by chemical analysis, of 1.5 (Fig. 10 (a-d)).

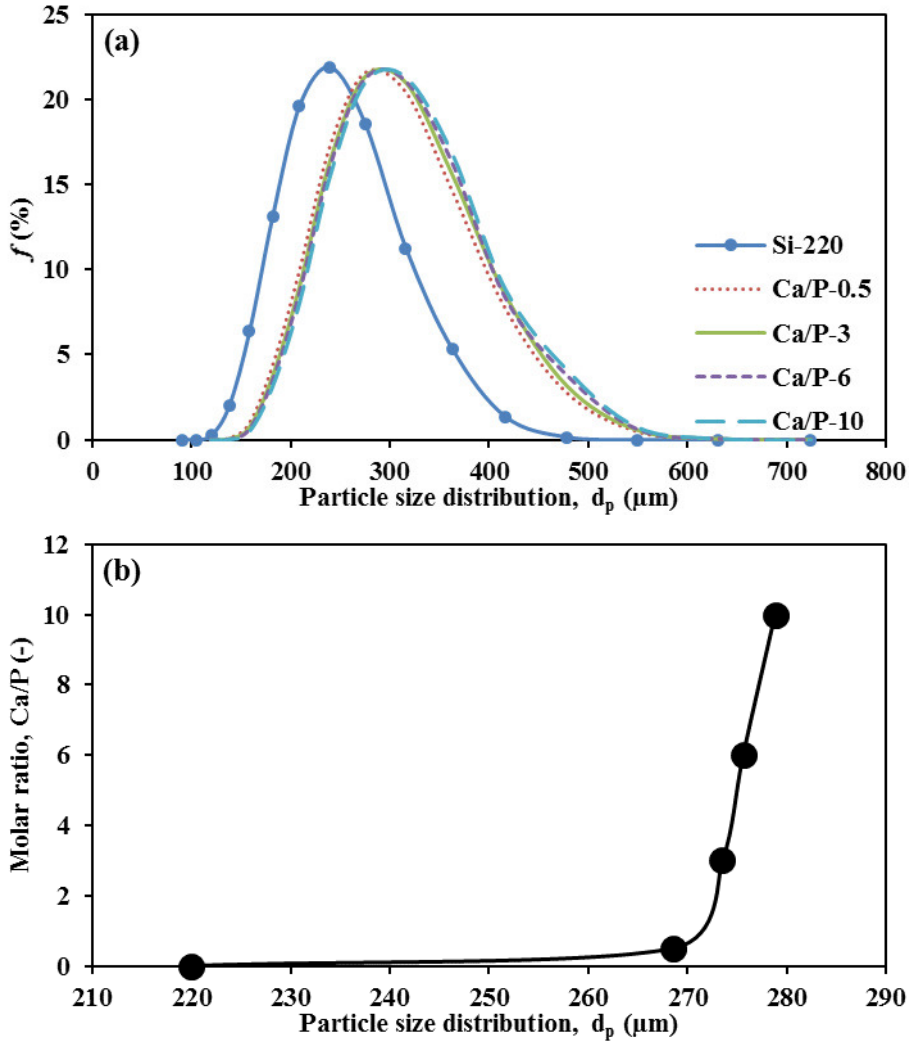


Figure 9. **a**) The particles size distribution of the sand before and after precipitation, **b**) change of $d_p$ as a function of Ca/P.

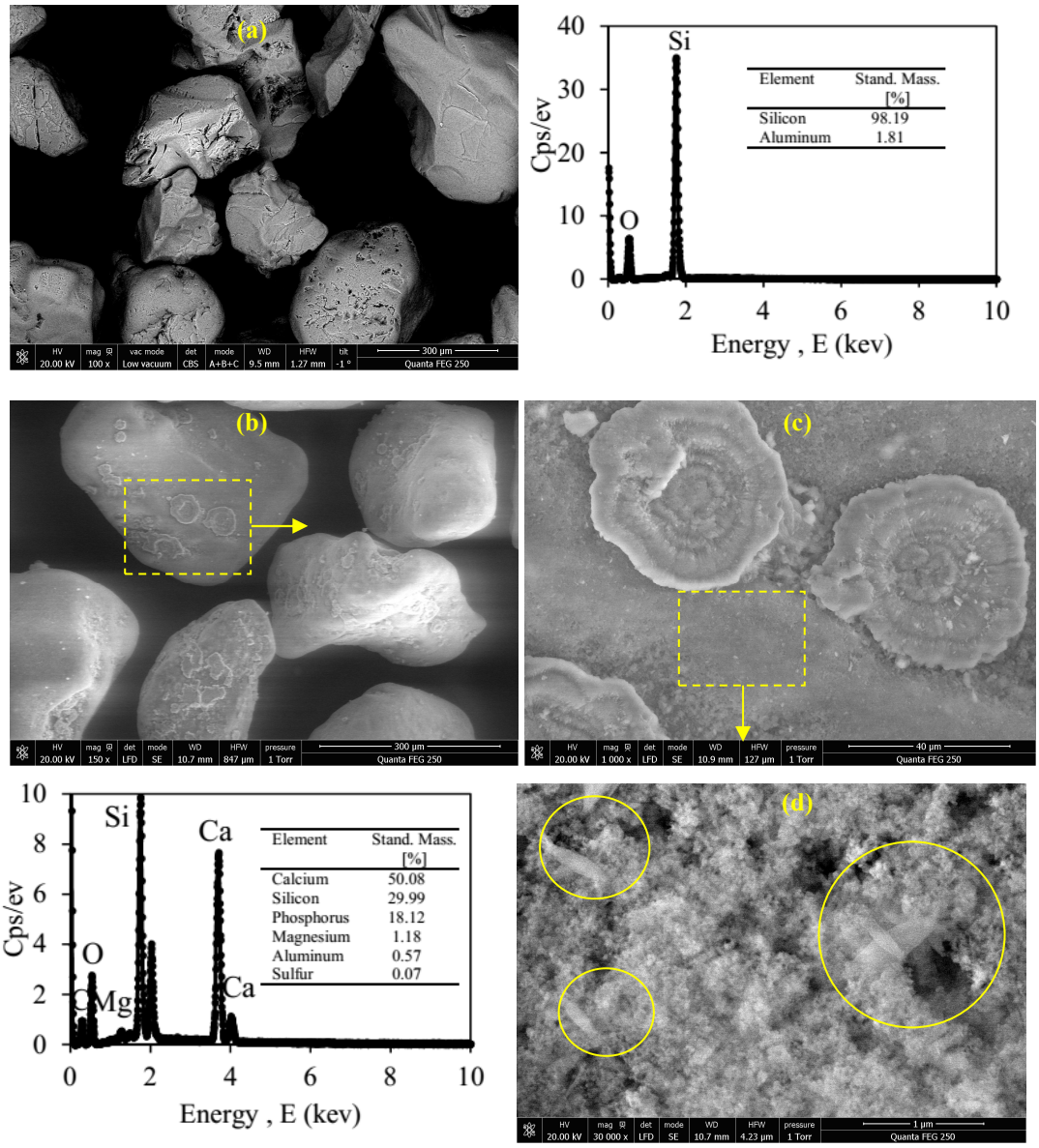


Figure 10. SEM images of sand particles surface, **(a)** before precipitation, **(b) (c) (d)** after precipitation, for the molar ratio Ca/P-6.

This result is in agreement with the analysis carried out Fourier transform infrared spectroscopy (FTIR). The spectra of the FTIR was obtained over the 600 to 4000 $cm^{-1}$. Figure 11 shows the FTIR spectra of the TCP, in which one of the characteristic absorption peaks of the $HPO_4^{2-}$ [28] was observed at 870 - 873 $cm^{-1}$.

Another characteristic peak of the $PO_4^{3-}$ bands at 603 and 1048 $cm^{-1}$ [28], [29]; however, a small amount of $CO_3^{2-}$ groups appeared as 873, 1415 and 1445 $cm^{-1}$ wave numbers [28], [29]. FTIR spectroscopy investigations showed distinct bands, which are characteristic for TCP, like Ca-P and Si-TCP. The complete list of the main vibration modes of TCP observed in figure 11 is shown in table 2.

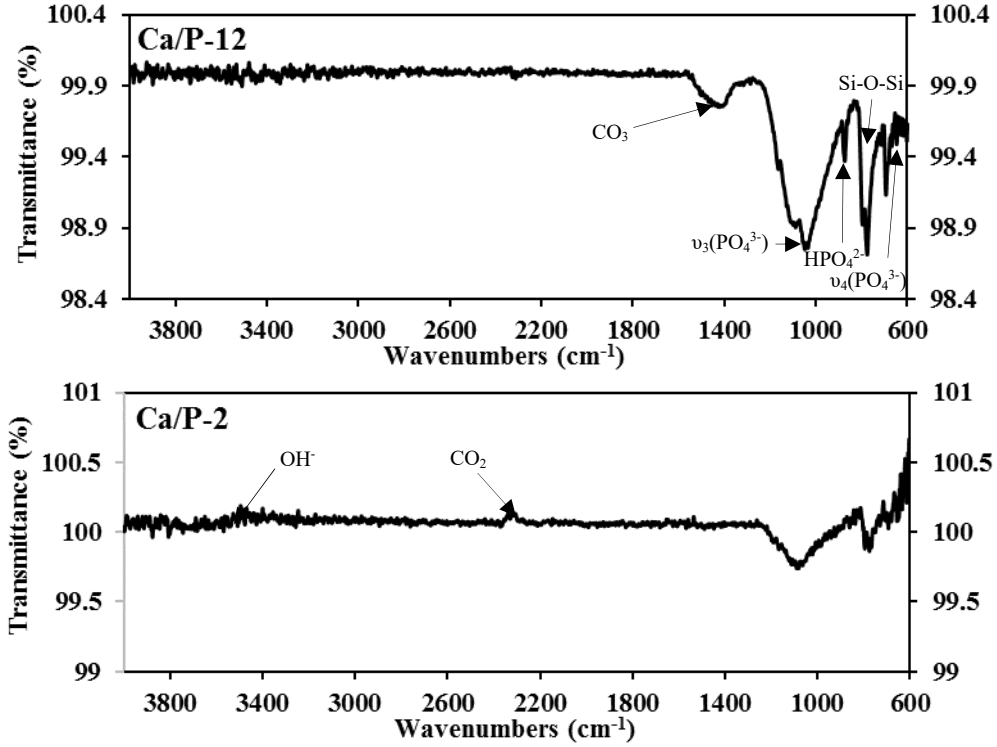


Figure 11. FTIR spectra of precipitated obtained for the value of the molar ratio (a) Ca/P-2 and (b) Ca/P-12.

Table 2. The absorption peak in the FTIR specter synthesized samples.

| Assignment | Frequency ($cm^{-1}$) | Refs |
|---|---|---|
| $PO_4^{3-}$ | 1037 – 1049, 1076 – 1080 | 27 |
| $HPO_4^{2-}$ | 870 – 873 | 27 |
| $CO_3^{2-}$ | 870 – 873, 1415, 1445 – 1450 | 27 |
| $OH^-$ | 630, 3566 | 27 |

As shown in figure 11 (a), the FTIR spectra illustrated an $OH^-$ ban **(b)** 453 $cm^{-1}$ and in figure 11(b), the band of $H_2O$ is observed at 630 $cm^{-1}$.

## 5. CONCLUSION

A hydrodynamic evaluation of the chemical precipitation of phosphates in FBR using $Ca(OH)_2$ was made. The efficiency of the chemical precipitation, as well as the quality of the precipitated products, is dependent on the water quality model utility and the operating conditions required.

Our experiments showed that the efficiency of phosphate recovery with sand and $Ca(OH)_2$ provides a cheaper alternative with a higher removal efficiency. At a molar ratio Ca/P≤4 and a phosphate concentration of 12.5 mgP/L, the recovery phosphate removal efficiency is 35~74% and an efficiency of 85~92% for a molar ratio Ca/P>4. The particle size dis **(a)** on of the sand particles before and after precipitation was observed to mean that the average diameter of the particles was increased to 36%.

It is found that the [Ca] and [$PO_4$] significantly affect the velocity of fluidization and the porosity of the fluidized bed. Parametric analysis of experimental results allowed us to propose a new correlation (Eq. 15) for predicting the expansion depending on the porosity of the bed. The error of equation 15 does not exceed 10%. SEM and FTIR analyzes have shown that the precipitate has a molar ratio greater than 1.5 and a chemical composition close to that of TCP.

## 6. ACKNOWLEDGEMENTS

We are grateful to the Industrial Process Engineering Department, University the Technology of Compiegne, France, for providing instrumentation facilities. The authors would like to acknowledge Pr. André PAUSS for his help.

## 7. REFERENCES

[1] C.C. Su, C.M. Chen, J. Anotai & M.C. Lu, 2013. Removal of Monoethanolamine and Phosphate from Thin-film Transistor Liquid Crystal Display (TFT-LCD) Wastewater by the Fluidized bed Fenton Process, *Chemical Engineering Journal*, Vol. 222, 128-135.

[2] S. Yeoman, T. Stephenson, J.N. Lester & R. Perry, 1988. The Removal of Phosphorus during Wastewater Treatment: A Review, *Environmental Pollution*, Vol. 49, 183-283.

[3] A. Alamdani & S. Rohani, 2007. Phosphate Recovery from Municipal Wastewater through Crystallization of Calcium Phosphate, *The pacific journal of science and technology*, Vol. 8(1), 27-31.

[4] C.C. Su, R.R.M. Abarca, M.D.G. de Luna & M.C. Lu, 2014. Phosphate Recovery from Fluidized Bed Wastewater by Struvite Crystallization Technology, *Journal of the Taiwan Institute of Chemical Engineers*, Vol. 45, 2395-2402.

[5] C. Trépanier, S. Parent, Y. Comeau & J. Bouvrette, 2002. Phosphorus Budget as a Water Quality Management Tool for Closed Aquatic Mesocosms, *Water Research*, Vol. 36, 1007-1017.

[6] L.E. De-Bashan & Y. Bashan, 2004. Recent Advances in Removing Phosphorus from Wastewater and its Future use as Fertilizer (1997–2003), *Water Research*, Vol. 38, 4222-4246.

[7] T.M. Wadood & A.R. Sarmad, 2012. Phosphorus Removal from Wastewater Using Oven-dried Alum Sludge, *International Journal of Chemical Engineering*, Vol. 2012, ID 125296, 11 p.

[8] R. Angel, 1999. Removal of Phosphate from Sewage as Amorphous Calcium Phosphate, *Environmental technology*, Vol. 20 (7), 709-720.

[9] A.T.K. Tran, Y. Zhang, D. De Corte, J.B. Hannes, W. Ye, P. Mondal, N. Jullok, B. Meesschaert, L. Pinoy & B.V.D. Bruggen, 2014. P-Recovery as Calcium Phosphate from Wastewater Using an Integrated Selectrodialysis/Crystallization Process, *Journal of Cleaner Production*, Vol. 77, 140-151.

[10] M.M. Seckler, O.S.L. Bruinsma & G.M. van Rosmalen, 1996. Calcium Phosphate Precipitation in a Fluidized Bed in Relation to Process Conditions: Black Box Approach, *Water Research*, Vol. 30, 1677-1685.

[11] W. Yi & K.V. Lo, 2003. Phosphate Recovery from Greenhouse Wastewater, *Journal of Environmental Science and Health*, Part B, Vol. 38, 501-509.

[12] N.Ö. Yigit & S. Mazlum, 2007. Phosphate Recovery Potential from Wastewater by Chemical Precipitation at Batch Conditions, *Environmental Technology*, Vol. 28, 83-93.

[13] G.K. Morse, S.W. Brett, J.A. Guy & J.N. Lester, 1998. Review: Phosphorus Removal and Recovery Technologies, *the Science of the Total Environment*, Vol. 212, 69-81.

[14] C.C. Su, L.D. Abarca Dulfo, M.L.P. Dalida & M.C. Lu, 2014. Magnesium Phosphate Crystallization in a Fluidized-Bed Reactor: Effects of pH, Mg:P Molar Ratio and Seed, *Journal Separation and Purification Technology*, Vol. 125, 90-96.

[15] Battistoni P., Fava G., Pavan P., Musacco A. & Cecchi F., 1997. Phosphorus Removal in Anaerobic Liquors by Strutive Crystallization without Addition of Chemicals: Preliminary Results, *Water Research*, Vol. 31, 2925-2929.

[16] Battistoni P., Passi B., Fatone F. & Pavan P., 2005. Phosphorus Removal from Supernatants at Low Concentration Using Packed and Fluidized Bed Reactors, *Industrial and Engineering Chemistry Research*, Vol. 44, 6701-6707.

[17] R. Aldaco, A. Garea & A. Irabien, 2007. Modeling of Particle Growth: Application Water Treatment in Fluidized Bed Reactor, *Chemical Engineering Journal*, Vol. 134, 66-71.

[18] Y. Shih, R.R.M. Abarca, M.D.G. de Luna, Y.-H. Huang, M.-C. Lu, 2017. Recovery of phosphorus from synthetic wastewaters by struvite crystallization in a fluidized-bed reactor: Effects of pH, phosphate concentration and coexisting ions, *Chemosphere*, Vol. 173, 466-473.

[19] J.F. Richardson & W.N. Zaki, 1997. Sedimentation and Fluidization, *Trans IChemE*, Vol. 75, S82-S100.

[20] A.M. Trushin, E.A. Dmitriev, M.A. Nosyrev & O.V. Kabanov, 2015. On the porosity of an Inhomogeneous Fluidized Bed, *Theoretical foundations of Chemical Engineering*, Vol. 49(6), 823-828.

[21] A. Guadie & S. Xia, 2012. Evaluating Factors Affecting Phosphorus Removal and Recovery from Wastewater Using Fluidized Bed Reactor, Proceeding of the 12th Symposium on Sustainable Water Resources Development, Arba Minch, 26-27 June 2012, AMU, Ethiopia, A special issue on *Ethiopian Journal of Water Science and Technology*, Vol. 12(1), 60-70.

[22] J. Christoffersen, M.R. Christoffersen, W. Kibalczyc & F.A. Andersen, 1989. A Contribution to the Understanding of the Formation of Calcium Phosphates, *Journal of Crystal Growth*, Vol. 94, 767-777.

[23] J.F. De Rooij, J.C. Heughebaert & G.H. Nancollas, (1984). A pH Study of Calcium Phosphate Seeded Precipitation, *Journal of Colloid and Interface Science*, Vol. 100 (2), 350-358.

[24] I. Lopez-Valero, C. Gomez-Lorente & R. Boistelle, 1992. Effect of Sodium and Ammonium Ions on Occurrence, Evolution and Crystallinity of Calcium Phosphates, *Journal of Crystal Growth*, Vol. 121, 297-304.

[25] F. Abonna & M. Franchini-Angela, 1990. Crystallization of Calcium and Magnesium Phosphates from Solutions of Low Concentration, *Journal of crystal Growth*, Vol. 104, 661-671.

[26] F. Abonna, H.E. Lundager Madsen & R. Boistelle, 1986. The Initial Phases of Calcium and Magnesium Phosphates Precipitated from Solutions of High to Medium Concentrations, *Journal of crystal Growth*, Vol. 74, 581-590.

[27] B. Formisani, R. Girimonte & T. Longo, 2008. The Fluidization Process of Binary Mixtures of Solids: Development of the Approach Based on the Fluidization Velocity Interval, *Powder Technology*, Vol. 185, 97-108.

[28] A. Gozalian, A. Behnamghader, M. Daliri & A. Moshkforoush, 2011. Synthesis and Thermal Behavior of Mg-Doped Calcium Phosphate Nanopowders via the Sol Gel Method, *Scientia Iranica F*, Vol. 18, 1614-1622.

[29] Farzadi A., Bakhshi F., Solati-Hashjin M., Asadi-Eydivand M. & abu Osman N., 2014. Magnesium incorporated hydroxyapatite: Synthesis and structural properties characterization, *Ceramics International*, Vol. 40, 6021-6029.